# Chapter 6

# BCS Phase Transition

At low enough temperatures a Fermi gas or electron-hole gas interacting with attractive forces undergoes a phase transition into the superfluid state. This is analogous to the phase transition exhibited by electrons into the superconducting state. There are two well-known paradigms for the superfluidity and superconductivity in a Fermi system:

(1) In a dense limit, the normal state is a degenerate Fermi liquid that undergoes a pairing instability at a temperature $k_B T_c \ll \varepsilon_F$. The formation of pairs and their condensation (macroscopic occupation at zero momentum state) both occur simultaneously at the critical temperature $T_c$.

(2) In a dilute limit, the bound states (composite bosons) form at some very high temperature $T_{\rm dissoc}$ and these preformed bosons then condense at the BEC critical temperature $T_c \ll T_{\rm dissoc}$.

In most cases of experimental interest, the system falls into one category or the other. For instance, $^3$He is a Fermi superfluid described by (1) while $^4$He is a superfluid described by (2). Essentially all cases of superconductivity in metals are much closer to (1) rather than (2). The theory of the transition of the type (1) was first introduced by Bardeen, Cooper and Schrieffer [1, 2] and is called the BCS phase transition. A pair of fermions with opposite momenta and spins forms a bound state which is referred to as a Cooper pair and behaves as a composite boson. These Bose particles exhibit Bose-Einstein condensation in the state of zero total momentum. This is the BCS scenario of the phase transition of type 1.

## 6.1 BEC-BCS crossover

It is of great interest to consider a model which interpolates between the above two regimes: the weak attraction in the high density limit is described by BCS theory of collective Cooper-pairs (momentum space pairing) while the strong attraction in the low density limit is described by BEC theory of tightly bound independent bosons (real-space pairing). There are experimental systems which may be in a regime intermediate between these two extreme limiting cases [3]. One such system is an exciton condensate in semiconductors

and the other is a high transition temperature superconductor in the copper-oxides.

Let us consider a bound pair of electron and hole in semiconductors, which is called an exciton [4]. The creation operator of an exciton with zero total momentum $K = 0$ is

$$\hat{b}_0^+ = \sum_k \varphi_k \hat{\alpha}_{k\uparrow}^+ \hat{\beta}_{-k\downarrow}^+, \tag{6.1}$$

where $\hat{\alpha}_{k\uparrow}^+ \equiv \hat{a}_{kc,\uparrow}^+$ is the creation operator of a conduction electron with momentum $k$ and up-spin, $\hat{\beta}_{k\downarrow}^+ \equiv \hat{a}_{kv,\uparrow}$ is the creation operator of a valance hole with momentum $-k$ and down-spin, which is equivalent to the destruction operator of a valance electron with momentum $k$ and up-spin, and $\varphi_k$ is the probability amplitude for an electron-hole pair excitation in a momentum space which is given by the Fourier transform of the relative wavefunction of an electron-hole pair. The modulus $|\varphi_k|$ extends from zero to the cut-off wavenumber $k \sim 1/a_B^*$, where $a_B^*$ is the Bohr radius of the exciton. If the coherent state of excitons is formed at the center-of-mass wavenumber $K = 0$ with a complex excitation amplitude $\psi$, such a state is generated by the translation operator starting from a vacuum state (crystal ground state):

$$\begin{aligned} |\psi\rangle = e^{\psi \hat{b}_0^+} |0\rangle &= e^{\psi \sum_k \varphi_k \hat{\alpha}_{k\uparrow}^+ \hat{\beta}_{-k\downarrow}^+} |0\rangle \\ &= \prod_k \left( u_k + v_k \hat{\alpha}_{k\uparrow}^+ \hat{\beta}_{-k\downarrow}^+ \right) |0\rangle, \end{aligned} \tag{6.2}$$

where the displacement operator $e^{\psi \sum_k \varphi_k \hat{\alpha}_{k\uparrow}^+ \hat{\beta}_{-k\downarrow}^+}$ is approximated by the first order expression $1 + \psi \sum_k \varphi_k \hat{\alpha}_{k\uparrow}^+ \hat{\beta}_{-k\downarrow}^+$. The variational parameter should satisfy $v_k/u_k = \psi \varphi_k$ at each momentum. The total number of Fermi particles (electrons and holes) in the system is $N = 2 \sum_k |v_k|^2$.

In a dilute limit in which an inter-exciton separation $d = n^{-1/3}$ is much larger than the Bohr radius $a_B^*$, the exciton behaves as a point boson and undergoes a usual Bose-Einstein condensation. The occupation number at each momentum eigenstate $|v_k|^2$ is much smaller than one as shown in Fig. 6.1(a), so that the Pauli exclusion principle does not play any role in the formation of BEC except for the fact that the repulsive interaction between excitons is ultimately traced back to the Pauli principle as well as the Coulomb force [4]. In other words the fermionic nature of electron and hole can be treated as a perturbation. The binding energy of an exciton $\Delta$ is much greater than the chemical potential $\mu \simeq -\Delta < 0$ in this regime, as shown in Fig. 6.1(b).

In an opposite dense limit, $n \geq 1/a_B^{*3}$, the electron-hole pairs strongly overlap so that the Pauli exclusion principle cannot be neglected. The occupation number $|v_k|^2$ cannot exceed one. Thus the constituent fermions (electrons and holes) must extend to higher momentum states in order to accommodate the total number $N$ of particles up to the Fermi momentum $\hbar k_F$ as shown in Fig. 6.1(a). The Fermions are normal except for a narrow window near the Fermi momentum, as will be discussed in the next section. The strong overlap of the constituent fermions decreases the binding energy $\Delta$ but a finite value of $\Delta$ still exists, which represents a cooperative interaction effect. The increase in the density results in the increase in the chemical potential $\mu$, which eventually overwhelms the binding energy $\Delta$ as shown in Fig. 6.1(b). In this limit, the weakly bound pairs of electrons and holes still exhibit Bose-Einstein condensation at low enough temperatures. This is the BCS phase transition.

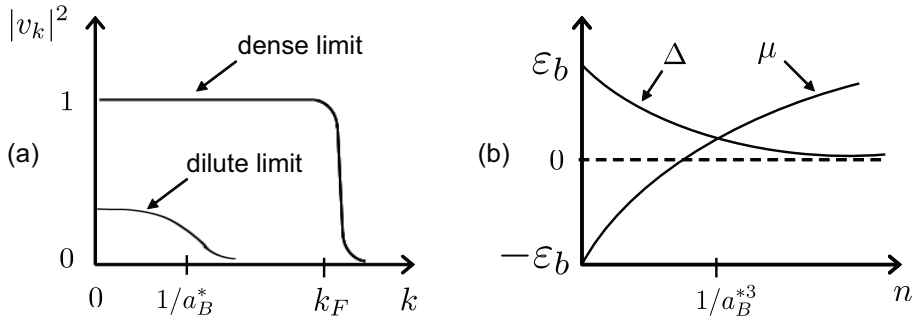


Figure 6.1: (a) The occupation number $|v_k|^2$ of each momentum eigenstate vs. wavenumber $k$ in dilute and dense limit. (b) The binding energy $\Delta$ and the chemical potential $\mu$ vs. composite particle density $n$. $\varepsilon_b$ is the exciton binding energy in a dilute limit.

In a small $n$ regime of Fig. 6.1(b), a normal BEC occurs at low enough temperatures. In the opposite limit of large $n$ regime of Fig. 6.1(b), a BCS phase is formed instead. The BEC-BCS crossover occurs when the chemical potential $\mu$ becomes positive and comparable to the binding energy $\Delta$ [4].

## 6.2 Bogoliubov transformation for Fermi particles

In this section we will review the basic features of the BCS formalism, in which a uniform Fermi gas has an attractive interaction potential. The system Hamiltonian has a form of

$$\hat{\mathcal{H}} = \sum_{p,s} \eta_p \hat{a}^+_{p,s} \hat{a}_{p,s} + \frac{g}{V} \sum_{p_1,p_2,p_1',p_2'} \hat{a}^+_{p_2'\uparrow} \hat{a}^+_{p_1'\downarrow} \hat{a}_{p_1\downarrow} \hat{a}_{p_2\uparrow}, \tag{6.3}$$

where $p_1 + p_2 = p_1' + p_2'$ and $V$ is the volume of the Fermi gas system. The energy of a free particle is defined with respect to the chemical potential,

$$\eta_p = \frac{p^2}{2m} - \mu. \tag{6.4}$$

Here the chemical potential is well approximated by the Fermi energy $\mu \simeq \frac{p_F^2}{2m}$, where $p_F$ is the Fermi momentum. The particle creation and annihilation operators satisfy the normal anti-commutation relations

$$\left\{ \hat{a}_{p,s}, \hat{a}^+_{p',s'} \right\}_+ = \delta_{pp'} \delta_{ss'}. \tag{6.5}$$

As mentioned already, the interaction is attractive ($g < 0$). The interaction is assumed to be independent of momenta between colliding Fermi particles.

The fact that the Fermi particle-pairs going into condensation have zero momentum permits us to simplify (6.3) by retaining only terms with $p_2 = -p_1 \equiv q$ and $p_2' = -p_1' \equiv p$. The reduced Hamiltonian is now

$$\hat{\mathcal{H}} = \sum_{p,s} \eta_p \hat{a}^+_{p,s} \hat{a}_{p,s} + \frac{g}{V} \sum_{p,q} \hat{a}^+_{p,\uparrow} \hat{a}^+_{-p,\downarrow} \hat{a}_{-q,\downarrow} \hat{a}_{q,\uparrow}. \tag{6.6}$$

The new Bogoliubov transformation is [5].

$$\hat{a}_{p,\uparrow} = u_p \hat{b}_{p,\uparrow} + v_p \hat{b}^+_{-p,\downarrow}, \tag{6.7}$$

$$\hat{a}_{p,\downarrow} = u_p \hat{b}^+_{p,\downarrow} - v_p \hat{b}_{-p,\uparrow}, \tag{6.8}$$

where $u_p$ and $v_p$, without loss of generality, have been chosen to be real. The annihilation and creation operators of the quasi-particles, $\hat{b}_{p,\uparrow}$ and $\hat{b}^+_{p,\uparrow}$, satisfy the Fermi anti-communication relation $\left\{\hat{b}_{p,s}, \hat{b}^+_{p',s'}\right\}_+ = \delta_{pp'}\delta_{ss'}$ if the modulus of $u_p$ and $v_p$ satisfy

$$u_p^2 + v_p^2 = 1 \tag{6.9}$$

The Hamiltonian (6.6) is diagonalized, i.e. all the off-diagonal terms vanish and the system energy $E$ is minimized, when $u_p^2$ and $v_p^2$ are chosen

$$u_p^2 = \frac{1}{2}\left(1 + \frac{\eta_p}{\sqrt{\Delta^2 + \eta_p^2}}\right), \tag{6.10}$$

$$v_p^2 = \frac{1}{2}\left(1 - \frac{\eta_p}{\sqrt{\Delta^2 + \eta_p^2}}\right). \tag{6.11}$$

Here the parameter $\Delta$ is determined by

$$-\frac{g}{2(2\pi\hbar)^3}\int dp \frac{1 - 2n_p}{\sqrt{\Delta^2 + \eta_p^2}} = 1, \tag{6.12}$$

where $n_p = \left\langle \hat{b}^+_{p,\uparrow}\hat{b}_{p,\uparrow}\right\rangle = \left\langle \hat{b}^+_{p,\downarrow}\hat{b}_{p,\downarrow}\right\rangle$ is the occupation number of the quasi-particle with momentum $p$. Equation (6.12) is called the "gap equation" because of the reason which will be discussed shortly. By virtue of the above transformation, the Hamiltonian (6.6) has the diagonal form

$$\hat{\mathcal{H}} = \sum_p \varepsilon_p \left(\hat{b}^+_{p,\uparrow}\hat{b}_{p,\uparrow} + \hat{b}^+_{p,\downarrow}\hat{b}_{p,\downarrow}\right), \tag{6.13}$$

with the Bogoliubov dispersion law given by

$$\varepsilon_p = \frac{\partial E}{\partial n_{ps}} = \sqrt{\Delta^2 + \eta_p^2}. \tag{6.14}$$

The excitation energy normalized by the Fermi energy is

$$\frac{\varepsilon_p}{\varepsilon_F} = \sqrt{\left[\frac{2\left(p - p_F\right)}{p_F}\right]^2 + \left(\frac{\Delta}{\varepsilon_F}\right)^2}, \tag{6.15}$$

where $\mu \simeq \varepsilon_F \simeq \frac{p_F^2}{2m}$ is used in (6.14). Equation (6.15) shows that the spectrum of the excitation energy features an energy gap $\Delta$ at the Fermi surface (at $p = p_F$) due to

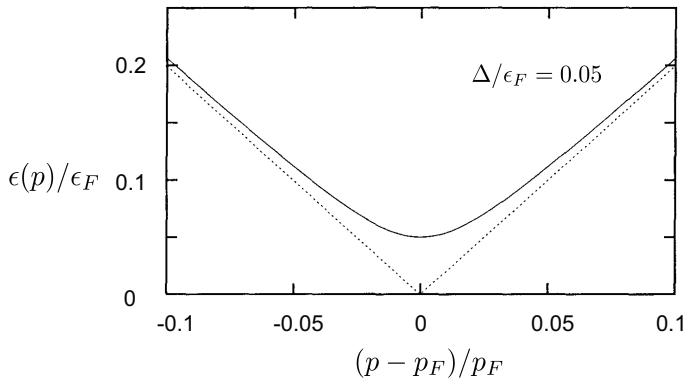


Figure 6.2: Quasi particle dispersion law (solid line) in a Fermi superfluid. The dotted lines give the prediction of the noninteracting Fermi gas.

the pairing mechanism, while the excitation spectrum of the non-interacting Fermi-gas is normal, $\eta_p = \frac{p^2}{2m} - \mu \simeq \frac{p_F}{m}(p - p_F)$, as shown in Fig. 6.2.

At zero temperatures, the population of the quasi-particles disappear, i.e. $n_p = 0$ and the gap can be calculated by

$$-\frac{g}{2(2\pi\hbar)^3}\int dp \frac{4\pi p^2}{\sqrt{\Delta_0^2 + \eta_p^2}} = 1, \tag{6.16}$$

which clearly shows that a solution for $\Delta_0$ exists only if $g < 0$, i.e. for attractive interactions. The solution of the above equation is approximately given by

$$\Delta_0 \simeq \varepsilon_F \exp\left(-\frac{2\pi^2\hbar^2}{m|g|k_F}\right) = \varepsilon_F \exp\left(-\frac{\pi}{2k_F|a|}\right), \tag{6.17}$$

where $a = \frac{m}{4\pi\hbar^2}g$ is the (negative) scattering length.

## 6.3 Superfluidity of Fermi systems

According to the Landau's criterion of superfluidity presented in the previous chapter, the change in energy due to the appearance of the excitation is $\varepsilon(\mathbf{p}) + \mathbf{p}\cdot\mathbf{v}$, where $\mathbf{p}, \varepsilon(\mathbf{p})$ and $\mathbf{v}$ are the momentum and the energy of the excitation and the velocity of the fluid. The spontaneous creation of excitations can take place only if it is energetically profitable, i.e.

$$\varepsilon(\mathbf{p}) + \mathbf{p}\cdot\mathbf{v} < 0. \tag{6.18}$$

This is possible if $v > \varepsilon(p)/p$ and the vectors $\mathbf{p}$ and $\mathbf{v}$ are opposite ($\mathbf{p}\cdot\mathbf{v} < 0$). If instead the velocity is smaller than the critical value

$$v_c = \min_p \frac{\varepsilon(p)}{p}, \tag{6.19}$$

no excitation will be created spontaneously and the fluid behaves as a superfluid.

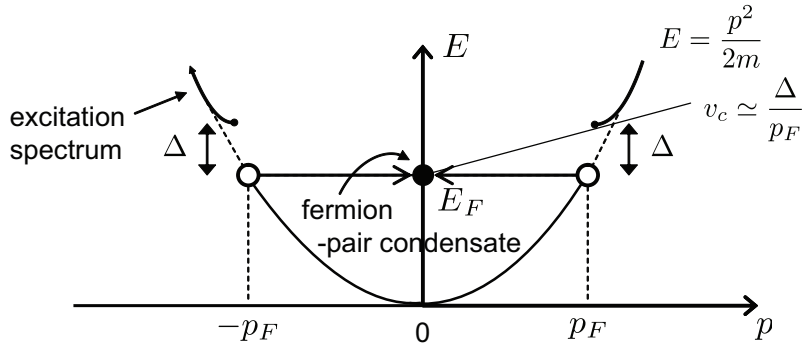


Figure 6.3: The energy gap $\Delta$ at the Fermi momentum $p_F$ and the critical velocity $v_c \simeq \frac{\Delta}{p_F}$ for superfluidity.

As shown in Fig 6.3, the above Landau's criterion for superfluidity is satisfied with a finite value of the critical velocity. Two fermions with opposite momenta $p_F$ and $-p_F$ form a Fermi-pair with zero net momentum and realizes Bose-Einstein condensation. If the condensate moves with a finite velocity satisfying

$$v < v_c \simeq \frac{\Delta}{p_F}, \tag{6.20}$$

(6.18) is not satisfied, so that no excitation is created and the Fermi-pair condensate features the superfluidity. This critical velocity is much smaller than the Fermi velocity $v_F = \frac{2E_F}{p_F}$, since the gap $\Delta$ is much smaller than the Fermi energy (see 6.17).

Similar to the phonon mode occurring for an interacting Bose gas, the density response of the Fermi gas in the BCS phase is characterized by a gapless phonon mode with the dispersion law $\omega = cp$, where $c$ is the sound velocity. The spreading in momentum of Fermi-pairs is of the order of $\delta p \sim \Delta/v_F$, which defines the healing length of Fermi superfluidity

$$\xi = \frac{\hbar}{\delta p} \simeq \frac{\hbar v_F}{\Delta}. \tag{6.21}$$

The size of quantized vortices in a superfluid Fermi gas is determined by this healing length, similar to the quantized vortices in a superfluid Bose gas. In general, due to the small size of $\Delta$, the healing length of the Fermi superfluid is significantly larger than the one of the Bose superfluid.

## 6.4 Critical temperature

At finite temperatures, the occupation number of the quasi-particles is given by the normal Fermi-Dirac distribution

$$n_p = \frac{1}{\exp\left(\varepsilon_p/k_B T\right) + 1}, \tag{6.22}$$

where the excitation energy $\varepsilon_p$ is measured from the Fermi energy. In the large momentum (or small gap) limit, $\varepsilon_p = \eta_p = \frac{p^2}{2m} - \mu$ and hence $n_p = \left\{\exp\left[\left(\frac{p^2}{2m} - \mu\right)/k_B T\right] + 1\right\}^{-1}$. Using this expression, one can solve the equation of the gap (6.12), at finite temperatures.

For sufficiently high temperatures, this equation does not have a solution for $\Delta$, reflecting that the system is no longer superfluid. The critical temperature $T_c$ at which the transition from the superfluid to the normal fluid takes place can be calculated by setting $\Delta = 0$ in (6.12). Equation (6.12) is reduced to

$$\log\left(\frac{\Delta_0}{\Delta}\right) = \int_{-\infty}^{\infty} \frac{d\eta_p}{\varepsilon\left(e^{\varepsilon/k_BT}+1\right)} = 2I\left(\Delta/k_BT\right), \tag{6.23}$$

where the integral $I\left(\Delta/k_BT\right)$ is expressed as,

$$I(u) = \int_0^{\infty} \frac{1}{\sqrt{x^2+u^2}} \cdot \frac{1}{\exp\left(\sqrt{x^2+u^2}\right)+1} dx. \tag{6.24}$$

At low temperature limits $k_BT \ll \Delta_0$, the gap decreases with the temperature exponentially:

$$\Delta = \Delta_0\left[1 - \sqrt{\frac{2\pi k_BT}{\Delta_0}} e^{-\Delta_0/k_BT}\right] \tag{6.25}$$

On the other hand, at high temperature limits $k_BT \lesssim \Delta_0$, (6.23) is simplified to

$$\log\left(\frac{\Delta_0}{\Delta}\right) = \log\left(\frac{\pi k_BT}{\delta\Delta}\right) + \frac{7\zeta(3)\Delta^2}{8\pi^2(k_BT)^2}. \tag{6.26}$$

The critical temperature $T_c$ is obtained by setting $\Delta = 0$ in (6.23) as

$$k_BT_c = \frac{\delta\Delta_0}{\pi} \sim 0.57\Delta_0, \tag{6.27}$$

where $\delta$ is the Euler constant. Substituting (6.27) into (6.26), the gap $\Delta$ near the critical temperature $T_c$ decreases with the temperature in the form of

$$\Delta = k_BT_c\left[\frac{8\pi^2}{7\zeta(3)}\left(1-\frac{T}{T_c}\right)\right]^{1/2} \sim 3.06k_BT_c\sqrt{1-\frac{T}{T_c}}. \tag{6.28}$$

Equations (6.17) and (6.27) for the gap at zero temperature and the critical temperature are based on the lowest-order Bogoliubov approximation [5, 6]. Taking the higher-order correction, the Fermi energy in (6.17) and (6.27) should be replaced by [7]

$$\varepsilon_F \to \frac{1}{2}\left(\frac{2}{e}\right)^{7/3}\varepsilon_F. \tag{6.29}$$

## 6.5 BEC-BCS crossover of exciton-polaritons

The Hamiltonian of the exciton-polariton system is given by

$$\hat{\mathcal{H}} = \hat{\mathcal{H}}_{exc} + \hat{\mathcal{H}}_{ph} + \hat{\mathcal{H}}_I, \tag{6.30}$$

where

$$\hat{\mathcal{H}}_{exc} = \sum_k \left\{ \left[ \frac{(\hbar k)^2}{2m_e} - \mu \right] \hat{\alpha}_k^+ \hat{\alpha}_k + \left[ \frac{(\hbar k)^2}{2m_h} - \mu \right] \hat{\beta}_k^+ \hat{\beta}_k \right\} + \frac{1}{2} \sum_{k,k',q} \Big[ V_q^{ee} \hat{\alpha}_{k'-q}^+ \hat{\alpha}_{k+q}^+ \hat{\alpha}_k \hat{\alpha}_{k'} + V_q^{hh} \hat{\beta}_{k'-q}^+ \hat{\beta}_{k+q}^+ \hat{\beta}_k \hat{\beta}_{k'} - 2V_q^{eh} \hat{\alpha}_{k+q}^+ \hat{\beta}_{k'-q} \hat{\beta}_{k'} \hat{\alpha}_k \Big], \tag{6.31}$$

$$\hat{\mathcal{H}}_{ph} = (\omega - \mu)\, \hat{a}^+ \hat{a}, \tag{6.32}$$

$$\hat{\mathcal{H}}_I = \Omega \sum_k \left( \hat{\alpha}_k^+ \hat{\beta}_{-k}^+ \hat{a} + \hat{a}^+ \hat{\beta}_{-k} \hat{\alpha}_k \right). \tag{6.33}$$

We assume the extended BCS wavefunction, consisting of a coherent state field and electron-hole excitation,

$$|\Phi\rangle = \exp\left(\lambda \hat{a}^+\right) \prod_k \left[ u_k + v_k \hat{\alpha}_k^+ \hat{\beta}_{-k}^+ \right] |0\rangle, \tag{6.34}$$

and then minimize the total energy (6.30) of the system in terms of the variational parameters $\lambda, u_k$ and $v_k$.

First, we switch-off the Coulomb interaction $\left(V_q^{ee} = V_q^{hh} = V_q^{eh} = 0\right)$. This simplified problem can be solved by the mean-field approximation. The relevant BCS equations are those for the excitation spectrum $E_k$, the mean field amplitude $\lambda$ and the total number of electron-hole pairs $D$:

$$E_k = \sqrt{\left( \frac{(\hbar k)^2}{2m} - \mu \right)^2 + (\Omega\lambda)^2}, \tag{6.35}$$

$$\lambda = -\frac{\Omega D}{\omega - \mu}, \tag{6.36}$$

$$D = -\sum_k \frac{\Omega\lambda}{2E_k} = \sum_k |v_k|^2. \tag{6.37}$$

Figure 6.4(a) shows the occupation probability $|v_k|^2$ of electron-hole states with wavenumber $k$ as a function of the normalized particle density $N = \left(\pi a_B^{*2}\right) n$. In a low density regime, a well-defined chemical potential $\mu$ exists, which is identified by the sharp cut-off of $|v_k|^2$. In an intermediate density regime (blue trace), the distribution of $|v_k|^2$ carries an uncertainty near the chemical potential. This is due to the electron-hole correlation induced by light-induced attractive interaction between them, which is analogous to the BCS state. However, in a high density regime (red trace), $|v_k|^2$ is saturated at $\sim 0.5$ over a wide range of wavenumbers. This is due to the coherent Rabi oscillation between the field and the electron-hole pair. Most of the system energy (or particles) is stored in the field rather than the electronic excitations as shown in Fig. 6.4(b) and (c) in a high density regime. The time averaged electron-hole pair is pinned at $|v_k|^2 = 0.5$ under the coherent Rabi oscillation induced by the strong field amplitude.

Next, we include the Coulomb interaction $V_q^{ee}, V_q^{hh}$ and $V_q^{eh}$ in (6.31). The occupation probability $|v_k|^2$ of electron-hole states with wavenumber $k$ is now shown in Fig. 6.5(a)

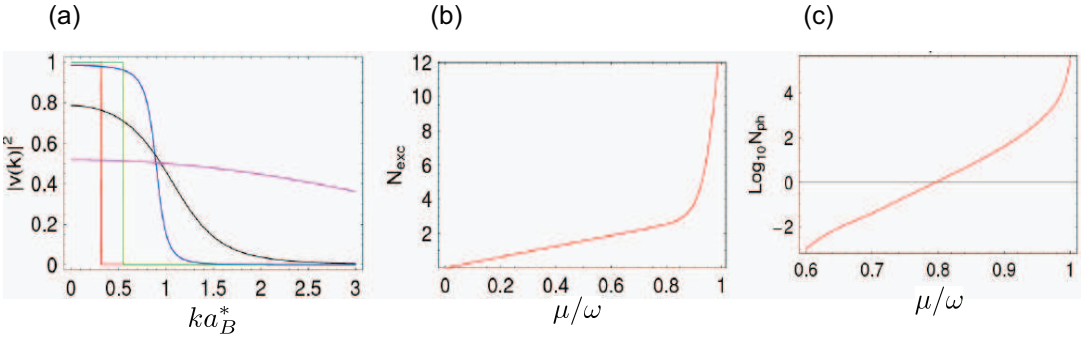


Figure 6.4: The solution of the BCS equations under the assumption: $V_q^{ee} = V_q^{hh} = V_q^{eh} = 0$. (a) $|v_k|^2$ vs. $ka_B^*$, (b) $N_{exc} = \sum_k |v_k|^2$ vs. $\mu/\omega$, and (c) $N_{ph} = |\lambda|^2$ vs. $\mu/\omega$.

as a function of $N = \left(\pi a_B^{*2}\right) n$. Note that in a low density regime, the distribution $|v_k|^2$ manifests the formation of a bound state (exciton) due to the attractive interaction $V_q^{eh}$. However, in a high density limit, the distribution $|v_k|^2$ is indistinguishable from that without the Coulomb interaction effect. The system is completely dominated by the coherent Rabi oscillation. Figure 6.5(b) shows $|v_k|^2$ vs. $ka_B^*$ when the coupling with the photon field is switched off, which corresponds to the standard BEC-BCS crossover in an exciton system. In this case, the Fermi liquid is normal $\left(|v_k|^2 = 1\right)$ below the chemical potential.

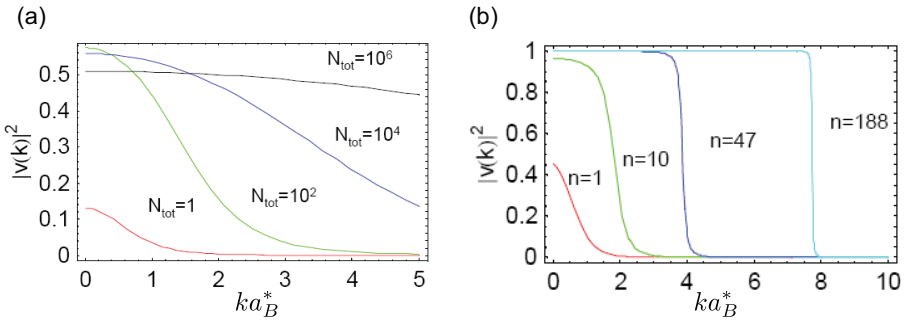


Figure 6.5: The occupation probability $|v_k|^2$ vs the normalized wavenumber $ka_B^*$ for (a) coupled exciton-photon system and (b) exciton system decoupled from photon field.

The BEC-BCS crossover in the exciton-polariton system is demonstrated in the numerical results shown in Fig. 6.6 [8]. When the chemical potential $\mu$ is far below the lower polariton energy, the conventional exciton-polariton splitting $2\Omega$ is observed for $\Delta = 0$ (zero detuning, Fig 6.6(a)) and a larger splitting $2\sqrt{\Omega^2 + \Delta^2/4}$ is observed for $\Delta > 0$ (blue detuning, Fig. 6.6(b)). When the chemical potential approaches to the lower polariton energy within $\sim k_B T$, the standard BEC occurs. A slight decrease in the exciton-polariton splitting is due to the phase space filling effect. If there is no coupling between the excitons and photons, the chemical potential continuously increases as shown by the dashed line. However, when there exists the coupling between the excitons and photons, most of the excitations is stored in the photon field and the increase in the chemical potential $\mu$ for the polariton system saturates. Simultaneously, the coherent Rabi oscillation induced by

the coherent field with an amplitude $\lambda$ opens up a gap $2\Omega\lambda$. This behavior is referred to as BEC-BCS crossover of exciton-polaritons [8].

The physics behind the exciton-polariton BCS is the coherent Rabi oscillation as mentioned above and so the triplet structure shown in Fig. 6.6 has a common root as the Mollow's triplet in atomic physics. On the other hand, the exciton BCS is a result of the screened and diminishing electron-hole Coumb attractive force [9, 10], so that its gap energy is much smaller than that of the exciton-polariton BCS. When a photon is absorbed and emitted by an electron-hole pair, the electron and hole must occupy the same lattice site. Otherwise, the dipole moment is not created. If the coherent Rabi oscillation (absorption and emission of photons) takes place very frequently, the electron-hole pairs become highly correlated in space like a Frenkel exciton even though their wavefunctions are strongly overlapped.

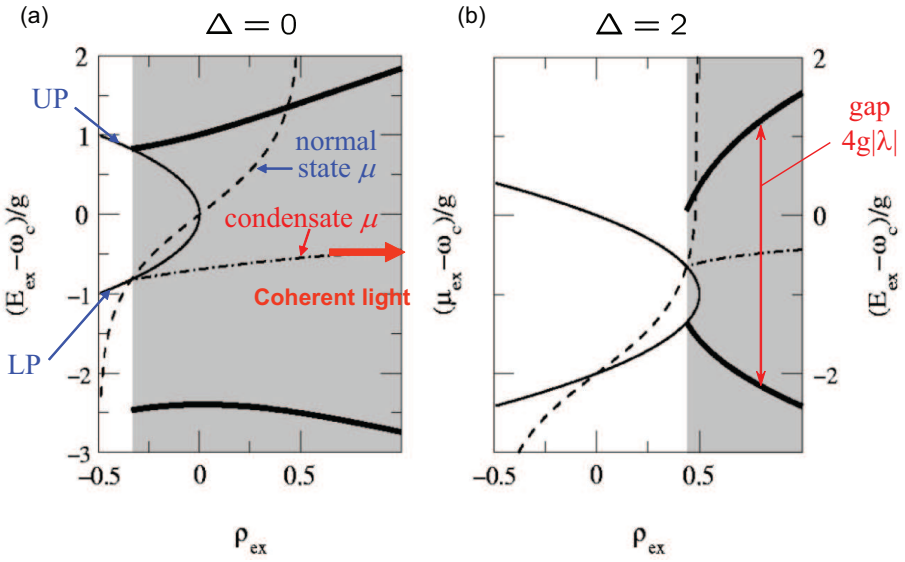


Figure 6.6: The BEC-BCS crossover of the exciton-polariton system. (a) $\Delta = 0$ (zero detuning), (b) $\Delta = 2$ (blue detuning).

# Bibliography


[1] J. Bardeen, L. N. Cooper, and J. R. Schrieffer. Microscopic theory of superconductivity. *Phys. Rev.*, 106:162–164, 1957.

[2] J. Bardeen, L. N. Cooper, and J. R. Schrieffer. Theory of superconductivity. *Phys. Rev.*, 108:1175–1204, 1957.

[3] A. J. Leggett. *Modern Trends in the Theory of Condensed Matter*. Springer-Verlag, Berlin, 1980. J. Phys. (Paris) Colloq, 41, C7.

[4] P. Nozieres and S. Schmitt-Rink. Bose condensation in an attractive fermion gas: From weak to strong coupling superconductivity. *J. Low Temp. Phys.*, 59:195, 1985.

[5] N. N. Bogoliubov. A new method in the theory of superconductivity 1. *Sov. Phys. JETP*, 7:41–46, 1958.

[6] N. N. Bogoliubov. On the theory of superfluidity. *J. Phys. (USSR)*, 11:23, 1947.

[7] L. P. Gorkov and T. K. Melikbarkhudarov. Structure of quantized vortex. *Sov. Phys. JETP*, 13:1018–1022, 1961.

[8] M. H. Szymanska and P. B. Littlewood. The crossover between lasing and polariton condensation in optical microcavities. *Solid State Communications*, 124:103, 2002.

[9] L. V. Keldysh and A. N. Kozlov. Collective properties of excitons in semiconductors. *Sov. Phys. JETP*, 27:521, 1968.

[10] C. Comte and P. Nozieres. Exciton Bose condensation - the ground state of an electron hole gas .1. mean field description of a simplified model. *J. Phys.*, 43:1069, 1982.